

Conjugated Polymers That Respond to Oxidation with Increased Emission

Eric L. Dane, Sarah B. King, and Timothy M. Swager*

Department of Chemistry, Massachusetts Institute of Technology, 77 Massachusetts Avenue, Cambridge, Massachusetts 02139

Received March 6, 2010; E-mail: tswager@mit.edu

Abstract: Thioether-containing poly(*para*-phenylene-ethynylene) (PPE) copolymers show a strong fluorescence turn-on response when exposed to oxidants in solution as a result of the selective conversion of thioether substituents into sulfoxides and sulfones. We propose that the increase in fluorescence quantum yield (Φ_F) upon oxidation is the result of both an increase in the rate of fluorescence (k_F), as a result of greater spatial overlap of the frontier molecular orbitals in the oxidized materials, and an increase in the fluorescence lifetime (τ_F), due to a decrease in the rate of nonradiative decay. Contrary to established literature, the reported sulfoxides do not always act as fluorescence quenchers. The oxidation is accompanied by spectral changes in the absorption and emission of the polymers, which are dramatic when oxidation causes the copolymer to acquire a donor–acceptor interaction. The oxidized polymers have high fluorescence quantum yields in the solid state, with some having increased photostability. A turn-on fluorescence response to hydrogen peroxide in organic solvents in the presence of an oxidation catalyst indicates the potential of thioether-containing materials for oxidant sensing. The reported polymers show promise as new materials in applications where photostability is important, where tunability of emission across the visible spectrum is desired, and where efficient emission is an advantage.

Introduction

Living in an oxidizing environment is essential for most life, but it has generally been an impediment to the use of fluorescent conjugated polymers (CPs) in practical applications. Fluorescent CPs are an important class of functional materials that have found use in applications ranging from organic light emitting diodes (OLEDs)¹ to the detection of TNT vapor at ppb levels via amplified fluorescence quenching.² Because most conjugated polymers become less emissive when oxidized, photobleaching attributed to reactions involving oxygen has limited their use.³ To better understand how to synthesize materials that are robust in our oxygen-rich atmosphere, we became interested in CPs that upon oxidation showed productive changes in emission, such as a large increase in emission, a significant shift in emission wavelength, or greater photostability.

Materials that show an increase in emission when oxidized are also candidates for the turn-on fluorescence sensing of peroxide oxidants. Being able to detect organic peroxides, such as triacetone triperoxide (TATP), is important because they can

be used to make dangerous explosive devices.⁴ On the other hand, hydrogen peroxide plays important biological roles, including being a disease marker and acting as a signaling molecule.⁵ Therefore, compounds that show an increase in fluorescence when oxidized by peroxides are important to the development of new sensing materials.

Previous studies on the photobleaching of fluorescent CPs have focused on understanding the mechanism. For example, fluorenone defects in polyfluorene act as low-energy trap sites that cause decreased emission intensity.⁶ In poly(*para*-phenylene-vinylene) (PPV) polymers, it has been suggested that the main degradation pathway involves the reaction of singlet oxygen with the alkenyl group, resulting in the formation of carbonyl defects that eventually result in chain scission.³ In poly(*para*-phenylene-ethynylene) (PPE)⁷ polymers, the mechanism of photobleaching has not been elucidated, but studies suggest that in model systems alkynes are less prone to reaction with singlet oxygen than alkenes.⁸ However, it is not clear that the observed photobleaching results solely from covalent bond

- (1) Grimsdale, A. C.; Chan, K. L.; Martin, R. E.; Jokisz, P. G.; Holmes, A. B. *Chem. Rev.* **2009**, *109*, 897–1091.
- (2) (a) Yang, Y.-S.; Swager, T. M. *J. Am. Chem. Soc.* **1998**, *120*, 5321–5322, and 11864–11873. (b) Thomas, S. W., III.; Joly, G. D.; Swager, T. M. *Chem. Rev.* **2007**, *107*, 1339–1386. (c) McQuade, D. T.; Pullen, A. E.; Swager, T. M. *Chem. Rev.* **2000**, *100*, 2537–2574.
- (3) (a) Scurlock, R. D.; Wang, B.; Ogilby, P. R.; Sheats, J. R.; Clough, R. L. *J. Am. Chem. Soc.* **1995**, *117*, 10194–10202. (b) Dam, N.; Scurlock, R. D.; Wang, B.; Ma, L.; Sundahl, M.; Ogilby, P. R. *Chem. Mater.* **1999**, *11*, 1302–1305.

- (4) (a) Malashikhin, S.; Finney, N. S. *J. Am. Chem. Soc.* **2008**, *130*, 12846–12847. (b) Schulte-Ladbeck, R.; Vogel, M.; Karst, U. *Anal. Bioanal. Chem.* **2006**, *386*, 559–565.
- (5) *Molecular Biology of Free Radicals in Human Diseases*; Aruoma, O. I., Halliwell, B. B., Eds.; OICA International: Micoud, St. Lucia, 1998.
- (6) (a) Romaner, L.; Pogantsch, A.; de Freitas, P. S.; Scherf, U.; Gaal, M.; Zojer, E.; List, E. J. W. *Adv. Funct. Mater.* **2003**, *13*, 597–601. (b) Cho, S. Y.; Grimsdale, A. C.; Jones, D. J.; Watkins, S. E.; Holmes, A. B. *J. Am. Chem. Soc.* **2007**, *129*, 11910–11911.
- (7) Bunz, U. H. F. *Chem. Rev.* **2000**, *100*, 1605–1644.
- (8) McIlroy, S. P.; Cló, E.; Nikolajsen, L.; Frederiksen, P. K.; Nielsen, C. B.; Mikkelsen, K. V.; Gothelf, K. V.; Ogilby, P. R. *J. Org. Chem.* **2005**, *70*, 1134–1146.

formation between the CPs and oxygen species, because in some cases it has been shown to be reversible.⁹ Although the specific mechanism is not known, CPs show greater photostability when irradiated under anaerobic conditions indicating that the presence of oxygen is important to photobleaching.¹⁰ Previous work from our group has found that antioxidants and triplet quenchers, such as cyclooctatetraene derivatives, can be added to thin films of CPs to attenuate photobleaching under irradiation.¹¹ Additionally, we have shown that polymers with high ionization potentials, due to the presence of electron-withdrawing perfluoroalkyl substituents, showed resistance to photobleaching.¹² Building on these previous investigations, this report focuses on designing CPs that respond positively to oxidation.

Previous examples of conjugated polymers where it was shown that oxidation did not cause a decrease in emission include polyfluorenes that contain small amounts of either a phosphafluorene or phosphafluorene oxide comonomer.¹³ Compared to the phosphine polymer's emission, the phosphine oxide polymer's emission was red-shifted in the solid state, but not in solution. However, the oxidized polymers had roughly the same emission efficiency as the unoxidized polymers, and in this example, the oxidation was carried out on the monomer before polymerization. We chose to append sulfur atoms, in the form of thioethers, directly to the polymer backbone because thioethers can be selectively oxidized in the presence of alkynes. In organic compounds, sulfur can have a formal oxidation state ranging from -2 to $+6$.¹⁴ In this investigation, we were interested in what effect changing the formal oxidation state from a thioether (-2) to that of a sulfoxide (0) or a sulfone ($+2$) would have on the photophysical properties of a PPE. Additionally, we hypothesized that the electron-withdrawing nature of the oxidized thioethers would lead to changes in absorption and emission wavelengths due to donor–acceptor interactions.

Conjugated polymers that contain sulfur atoms are ubiquitous in materials chemistry, but almost exclusively the sulfur atom is contained in a thiophene ring.¹⁵ Surprisingly, we can find relatively few examples of the incorporation of thioethers into CPs, though a review by Gingras¹⁶ summarizes how chemists have exploited the properties of persulfurated aromatic compounds. Lehn¹⁷ synthesized a series of diacetylene-linked poly(phenylthio)-substituted benzenes that showed the ability to be multiply reduced, taking advantage of sulfur's ability to stabilize a negative charge. Additionally, several examples of thioether-containing PPV CPs have been reported.¹⁸ In general, aromatic sulfones, and especially aromatic sulfoxides, have not been extensively utilized in materials chemistry.

We designed a monomer that contains four thioethers divided between two dithiolane rings. Because the sulfur atoms of **1** (Scheme 1) are not members of an aromatic ring system, it was anticipated that they would behave differently than a sulfur atom in a thiophene ring system. The five-member rings have the advantage of tying back the sulfur atoms ($\theta_{\text{CCS}} = 123^\circ\text{--}124^\circ$; see Scheme 1, X-ray structure of **1**) and minimizing their steric interference with the reactive positions used in polymerization. Additionally, they allow for the facile introduction of solubilizing groups from readily available symmetrical and asymmetrical ketones via acid-catalyzed condensation. It was anticipated that the branching of the aliphatic solubilizing groups would aid in solubility and prevent aggregation in the solid state. Monomers and polymers with a similar geometry with oxygen in place of sulfur have been recently described.¹⁹

Results

Synthesis. Monomer **1** is available in three steps from inexpensive starting materials without the need for chromatography. Compound **2** was synthesized via complete nucleophilic aromatic substitution of 1,2,4,5-tetrachlorobenzene with sodium 2-methylpropane thiolate in refluxing dimethylformamide, followed by recrystallization from refluxing methanol (59% yield).²⁰ The *tert*-butyl groups were deprotected *in situ*, and the resulting thiols were condensed with 5-nonanone in the presence of $\text{HBF}_4 \cdot \text{Et}_2\text{O}$ in refluxing toluene. Compound **3** could not be successfully brominated or iodinated via electrophilic substitution, presumably due to nucleophilic attack by the thioethers on the electrophilic reagents and subsequent side reactions. Rather than pursue a method of sequential lithiations, we used an excess of lithium tetramethylpiperidine and chlorotrimethylsilane to drive the double deprotonation of **3** to completion in one flask.²¹ The resulting ditrimethylsilyl product was carried through to be iodinated with ICl in CH_2Cl_2 . Monomer **3** was purified by recrystallization from hexane and obtained in an overall yield of 38% as an air-stable yellow solid.

Model compounds (**MC1** and **MC2**) and polymers (**P1** and **P2**) were synthesized via Sonagashira cross-coupling in good yield. **P1** was isolated as a high molecular weight polymer ($M_n = 236\,000$ g/mol) according to gel permeation chromatography (GPC) and was soluble in common organic solvents such as CH_2Cl_2 and THF. Under the same conditions, **P2** formed high molecular weight polymers that became insoluble, either because with increased chain length the polymers become insoluble or because of the presence of cross-linking. To isolate soluble polymers, the temperature of the polymerization was lowered from 65 to 45 °C. At the lower reaction temperature, the molecular weight of **P2** ($M_n = 18\,900$ g/mol) decreased and the isolated polymer was soluble. In addition to GPC, the polymers were characterized by ^1H and ^{13}C NMR and FT-IR.

Oxidation of Model Compounds. Model compounds **MC1** and **MC2** were oxidized with 1 and 2 equiv of *m*-chloroper-

(9) Park, S.-J.; Gesquiere, A. J.; Yu, J.; Barbara, P. F. *J. Am. Chem. Soc.* **2004**, *126*, 4116–4117.

(10) (a) Yan, M.; Rothberg, L. J.; Papadimitrakopoulos, F.; Galvin, M. E.; Miller, T. M. *Phys. Rev. Lett.* **1994**, *73*, 744–747. (b) Kocher, C.; Montali, A.; Smith, P.; Weder, C. *Adv. Funct. Mater.* **2001**, *11*, 31–35.

(11) Andrew, T. L.; Swager, T. M. *Macromolecules* **2008**, *41*, 8306–8308.

(12) (a) Kim, Y.; Swager, T. M. *Chem. Commun.* **2005**, 372–374. (b) Kim, Y.; Whitten, J. E.; Swager, T. M. *J. Am. Chem. Soc.* **2005**, *127*, 12122–12130.

(13) Chen, R.-F.; Zhu, R.; Fan, Q.; Huang, W. *Org. Lett.* **2008**, *10*, 2913–2916.

(14) McNaught, A. D.; Wilkinson, A. *IUPAC Compendium of Chemical Terminology*, 2nd ed.; Blackwell Science, 1997.

(15) Roncali, J. *Chem. Rev.* **1992**, *92*, 711–738.

(16) Gingras, M.; Raimundo, J.-M.; Chabre, Y. M. *Angew. Chem., Int. Ed.* **2006**, *45*, 1686–1712.

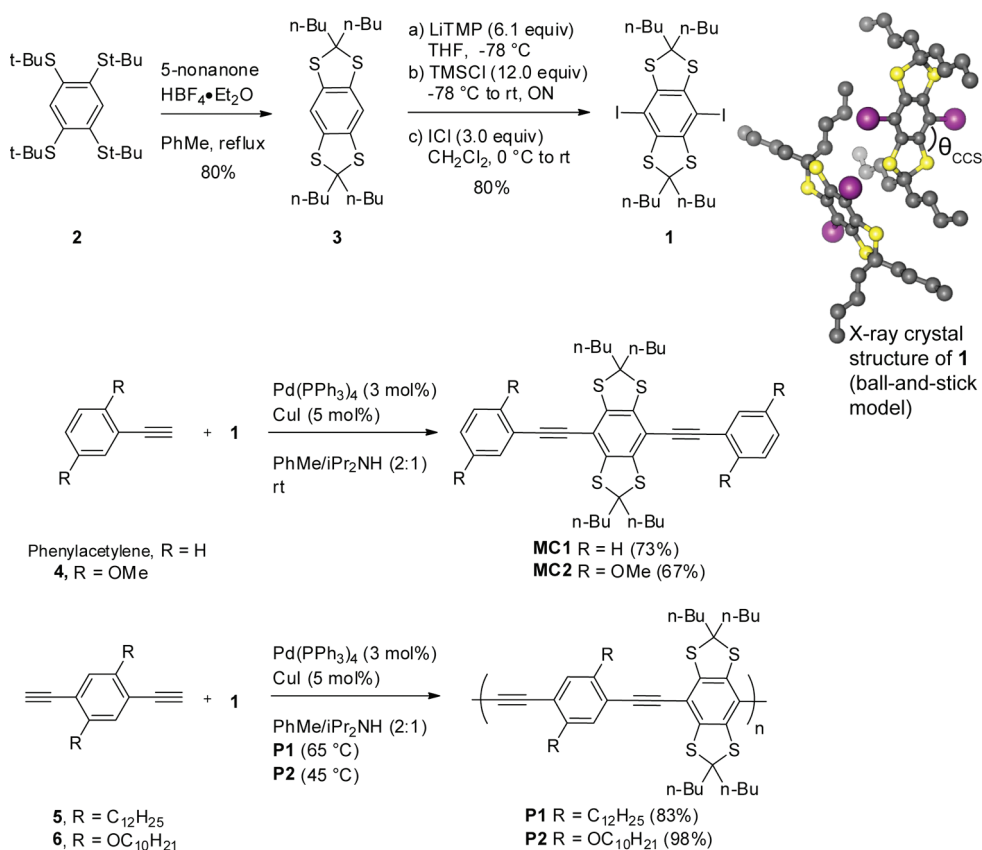
(17) Mayor, M.; Lehn, J.-M.; Fromm, K. M.; Fenske, D. *Angew. Chem., Int. Ed. Engl.* **1997**, *36*, 2370–2372.

(18) (a) Yoon, C.-B.; Kang, I.-N.; Shim, H.-K. *J. Polym. Sci., Part A: Polym. Chem.* **1997**, *35*, 2253–2258. (b) Shim, H. K.; Yoon, C. B.; Ahn, T.; Hwang, D. H.; Zyung, T. *Synth. Met.* **1999**, *101*, 134–135. (c) Reisch, H. A.; Scherf, U. *Macromol. Chem. Phys.* **1999**, *200*, 552–561. (d) Hou, J.; Fan, B.; Huo, L.; He, C.; Yang, C.; Li, Y. *J. Polym. Sci., Part A: Polym. Chem.* **2006**, *44*, 1279–1290. (e) Gutierrez, J. J.; Luong, N.; Zepeda, D.; Ferraris, J. P. *Polym. Prepr. (Am. Chem. Soc., Div. Polym. Chem.)* **2004**, *45*, 172–173.

(19) Dutta, T.; Woody, K. B.; Parkin, S. R.; Watson, M. D.; Gierschner, J. *J. Am. Chem. Soc.* **2009**, *131*, 17321–17327.

(20) Reddy, T. J.; Iwama, T.; Halpern, H. J.; Rawal, V. H. *J. Org. Chem.* **2002**, *67*, 4635–4639.

(21) Krizan, T. D.; Martin, J. C. *J. Am. Chem. Soc.* **1983**, *105*, 6155–6157.

Scheme 1. Preparation of **1**, **MC1**, **MC2**, **P1**, and **P2**

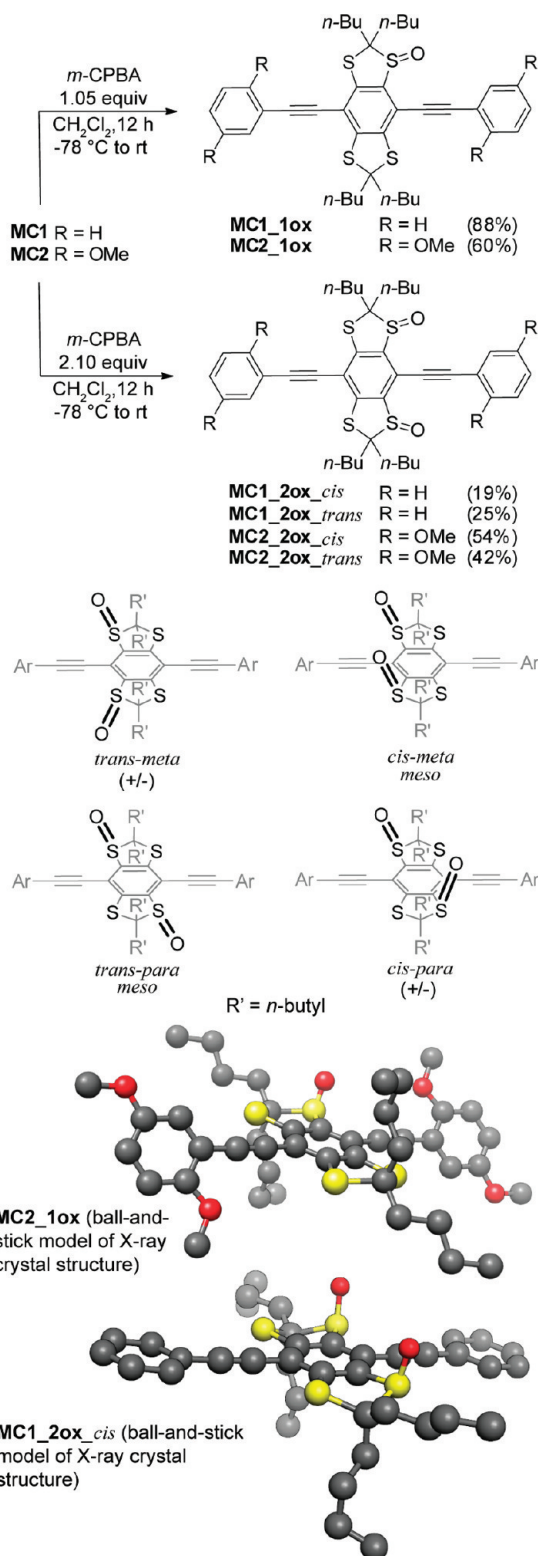
benzoic acid, and the mono- and disulfoxides of each (**MC1_1ox**, **MC1_2ox**, **MC2_1ox**, and **MC2_2ox**) were isolated (Scheme 2). The mono- and disulfoxides were characterized with ^1H and ^{13}C NMR, FT-IR, and HRMS. For **MC2_1ox** and **MC1_2ox_cis**, X-ray crystallography was used to ensure the identity of the compound (see Supporting Information for ORTEP diagrams). For each of the disulfoxides, four diastereomers were obtained (Scheme 2). The *cis*-isomers, in which the polar sulfoxide bonds point in the same direction and increase the overall dipole of the molecule, had a significantly longer retention time on silica gel as compared to the *trans*-isomers, in which the dipoles point in opposite directions. The two isomers were easily separated via chromatography. As expected, the directing influence of the thioethers favored a *meta*-orientation for the sulfoxides over a *para*- or an *ortho*-relationship, although a small amount of *para*-compound was observed in each case. The *meta*- and *para*-isomers show diagnostic ^1H and ^{13}C NMR, with the *para*-isomer having fewer unique ^1H and ^{13}C signals because of its higher symmetry. For **MC1_2ox**, the *cis*- and *trans*-products contained less than 10% of the *para*-isomer according to integration of the proton NMR. For **MC2_2ox**, the isolated *cis*- and *trans*-products contained the *meta*- and *para*-isomer in a ratio of roughly 3:1. The selectivity for the second oxidation to occur at the *meta*-position as opposed to the *para*-position results from the first sulfoxide withdrawing electron density from the sulfur atoms in an *ortho*- and *para*-orientation more effectively than from the sulfur in a *meta*-orientation. The *ortho*-compound was not observed. The oxidation of the second sulfur in dithioacetals is often much

slower as compared to the oxidation of the first, with the oxidation of the sulfoxide to sulfone as a competing process.²²

Optical and Photophysical Properties of the Model Compounds in Solution. Both **MC1** and **MC2** have similar absorbance and emission properties (see Table 1, Figure 1) in solution (CH_2Cl_2). **MC1** and **MC2** have strong absorbance peaks between 300 and 400 nm, with a weaker absorbance between 400 and 500 nm. The absorbance maxima for **MC2** (375 nm) is red-shifted as compared to **MC1** (355 nm), as a result of the electron-donating methoxy groups at the 1- and 4-positions of the outer aryl rings. However, the same effect is not seen in the less intense band in the visible region, where the absorbance maximum of **MC1** (434 nm) is nearly the same as that of **MC2** (435 nm). **MC1** and **MC2** are relatively nonemissive, with quantum yields (Φ_F) of less than 0.01, and they show broad, featureless emission centered near 490 nm.

Interestingly, when thoroughly degassed with bubbling nitrogen, both **MC1** and **MC2** show an additional sharp, red-shifted emission peak (**MC1**, 560 nm; **MC2**, 580 nm) and a vibronic shoulder above 600 nm (see Figure S1 in Supporting Information). Exposure of the samples to air causes the peak to completely disappear. Quenching of the emission by oxygen indicates that the emissive process involves an excited triplet state rather than a singlet state. Room temperature phosphorescence is unusual for organic compounds of this type, and it indicates that the four thioether substituents on the central

(22) Aggarwal, V. K.; Davies, I. W.; Franklin, R.; Maddock, J.; Mahon, M. F.; Molloy, K. C. *J. Chem. Soc., Perkin Trans. 1* **1994**, 2363–2368.

Scheme 2. Oxidation of **MC1** and **MC2**

aromatic ring promote intersystem crossing from the singlet excited state to triplet excited state.²³

For both **MC1** and **MC2**, oxidation to the monosulfoxide causes an increase in Φ_F relative to the parent compound, with the effect being more dramatic for **MC2**. This increase in Φ_F

is accompanied by a blue shift in emission, which is more pronounced for **MC1**. The emission maximum of **MC1** shifts from 489 nm for the unoxidized version to 458 nm for the monosulfoxide (**MC1_1ox**). The emission maximum of **MC2** shifts from 493 nm for the unoxidized version to 467 nm for the monosulfoxide (**MC2_1ox**). Further oxidation of **MC1_1ox** to **MC1_2ox** does not cause a significant change in Φ_F ; however it is accompanied by a shift in emission maximum from 458 to 403 nm and a change in the structure of the emission. Conversely, further oxidation of **MC2_1ox** to **MC2_2ox** results in a 10-fold increase in fluorescence quantum yield and is accompanied by a small red shift of the emission maximum from 467 to 474 nm. As discussed in the previous section, *cis*- and *trans*-isomers of **MC1_2ox** and **MC2_2ox** were isolated and characterized separately. There appears to be no significant difference in the photophysical properties of the *cis*- and *trans*-isomers. However, it should be noted that in all cases we isolated the *cis*- and *trans*-isomers as a mixture of regioisomers. Because the compounds were not separated, we cannot comment on how the *meta*- versus *para*-orientation of the sulfoxides affects the photophysical properties.

To investigate the effect of further oxidation, we observed the absorbance and emission changes caused by adding increasing amounts of *m*-CPBA to dilute solutions of **MC1** and **MC2** (see Figure S2 in Supporting Information). Increasing oxidation of **MC1** is accompanied by blue-shifted absorbance and emission and a general increase in emission. Comparison of the spectrum with those of isolated compounds indicates that, after the initial formation of **MC1_1ox**, a significant amount of **MC1_2ox** is formed. Additionally, a peak emerges at 422 nm that we attribute to sulfone-containing compounds with significantly higher quantum yields than the sulfoxides.²⁴ When **MC2** is titrated with oxidant, there is an initial blue shift in absorbance and emission, also accompanied by a substantial increase in emission. However, as the compound is further oxidized the donor–acceptor interaction that develops between the electron-rich terminal aromatic rings and the increasingly electron-poor center ring causes a red shift in absorbance and emission. The red shift in emission is accompanied by a decrease in emission efficiency; however the resulting fluorophores are still substantially more emissive than the parent compound.

Oxidation of Polymers. Polymers **P1** and **P2** were oxidized with 2.10, 3.15, 4.20, 6.30, and 8.40 equiv of *m*-CPBA overnight at room temperature in a CH_2Cl_2 solution (Figure 2, **P1A–D** and **P2A–D**). The oxidation products of **P1** did not show substantial changes in color; however the reaction mixtures became noticeably green fluorescent under ambient light. Conversely, the color of **P2** changed from yellow to red with increasing amounts of oxidation. The effect of the oxidation on molecular weight was monitored with GPC and is summarized in Table 2. The M_n of the polymers decreased with greater amounts of oxidation. The addition of 8.4 equiv of oxidant caused the molecular weight of **P1** to decrease by half. This suggests that oxidation at the alkyne linkages becomes more competitive with sulfur oxidation with higher amounts of oxidant. It has been reported that diphenylacetylene slowly reacts

(24) To understand the effect of sulfone formation, **MC1** was treated with 8.0 equiv of *m*-CPBA in refluxing CH_2Cl_2 overnight. The least polar fractions were separated by chromatography. The mixture obtained showed strong sulfone signals in FT-IR, an absorption maximum at 392 nm, and a broad emission with a maximum near 414 nm. The sulfone-containing compounds are also much more emissive than the sulfoxides, with an average quantum yield of 0.40 measured at several excitation wavelengths between 350 and 380 nm.

(23) Turro, N. J. *Modern Molecular Photochemistry*; University Science Books: Sausalito, CA, 1991.

Table 1. Model Compound Photophysics in CH₂Cl₂

compound	λ_{max} (nm)/ ϵ (M ⁻¹ ·cm ⁻¹)	λ_{em} (nm)	Φ_{F}^a	τ_{F} (ns)	k_{F}^e (ns ⁻¹)
MC1	355 (28 000), 372 (24 000), 434 (4600)	489	0.0030	0.094 ^b	0.032
MC1_1ox	304 (35 000), 353 (26 000), 422 (7600)	458	0.029	<0.4 ^{b,c}	>0.07 ^c
MC1_2ox_cis	308 (38 000), 358 (22 000)	403	0.038	<0.5 ^{b,c}	>0.08 ^c
MC1_2ox_trans	309 (38 000), 360 (21 000)	403	0.022	<0.4 ^{b,c}	>0.06 ^c
MC2	375 (22 000), 435 (4500)	493	0.0030	0.099 ^b	0.030
MC2_1ox	308 (23 000), 381 (20 000)	467	0.055	2.7 ^d	0.020
MC2_2ox_cis	310 (25 000), 387 (18 000)	473	0.62	2.9 ^d	0.21
MC2_2ox_trans	310 (26 000), 387 (17 000)	473	0.52	2.9 ^d	0.18

^a Absolute quantum yields were determined by comparison with 9,10-diphenylanthracene in cyclohexane ($\Phi_{\text{F}} = 0.90$). ^b Fluorescence lifetimes were measured using a pulsed-femtosecond laser (350 nm) and were fit to monoexponential decays with $R^2 > 0.99$. ^c Obtained lifetimes could be fit to monoexponential decays, but the emission profile suggested that photodegradation via deoxygenation to the sulfide occurred during excitation. Therefore, only an upper bound is placed on the lifetime, and a minimum k_{F} is calculated. ^d Fluorescence lifetimes were measured using a pulsed-picosecond laser (415 nm) and were fit to monoexponential decays with $R^2 > 0.99$. ^e $\Phi_{\text{F}}/\tau_{\text{F}}$.

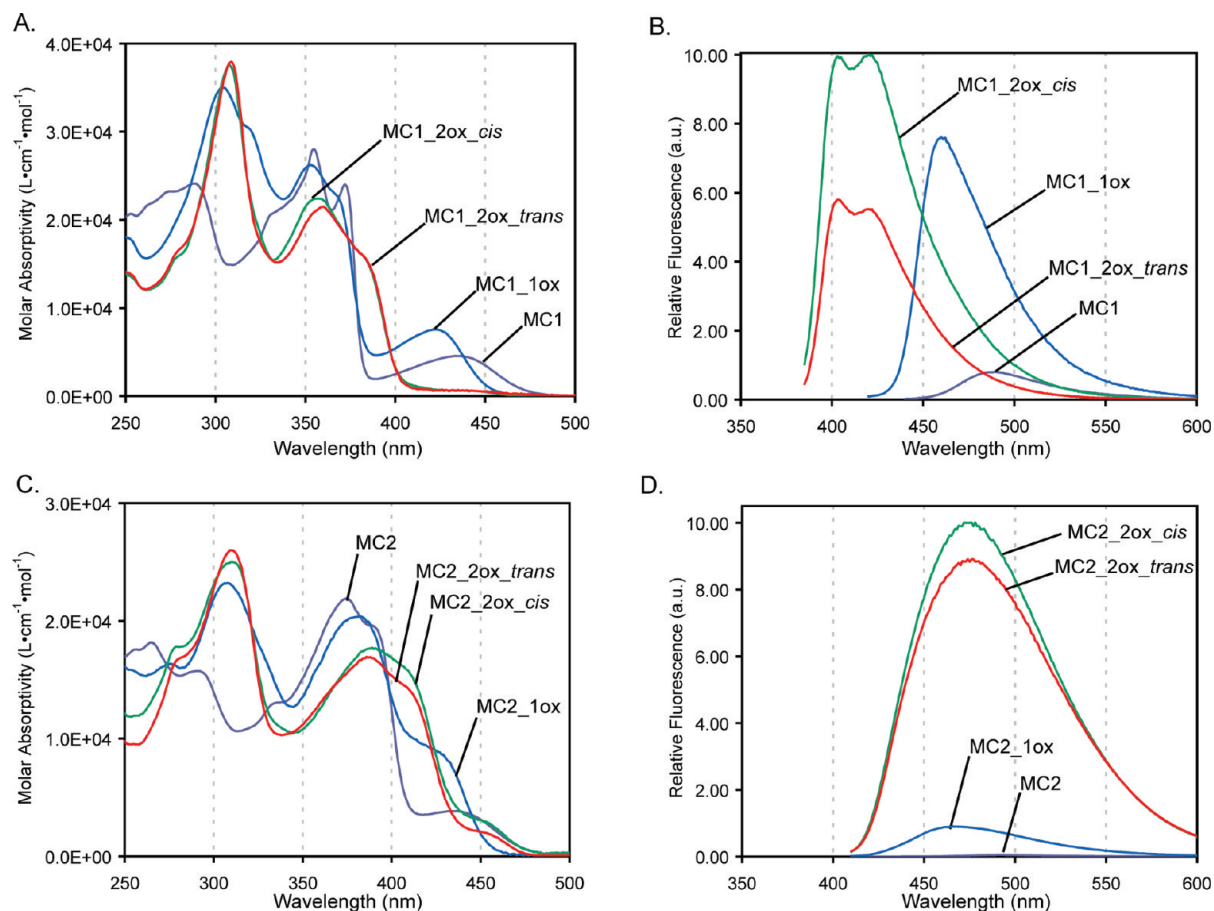


Figure 1. Model compound oxidation. (a and c) The absorption spectra of **MC1**, **MC2**, and oxidation products. (b and d) The fluorescence spectra of **MC1**, **MC2**, and oxidation products. Within each plot, the fluorescence intensity is scaled to reflect the relative emissivity of each fluorophore as determined by its absolute quantum yield (see Table 1 for values). λ_{ex} : 420 nm (**MC1**, **MC2**), 390 nm (**MC1_1ox**, **MC2_1ox**, **MC2_2ox**), 370 nm (**MC1_2ox**). All spectra were taken in CH₂Cl₂, and all fluorescence spectra are corrected for PMT response.

with *m*-CPBA in chloroform at room temperature to give a variety of oxidation products resulting from the initial formation of an oxirene.²⁵ Some of the oxidation products reported result in cleavage of the diphenylacetylene into two molecules, while others contain linkages that are susceptible to cleavage.²⁵

The presence and relative abundance of sulfoxides and sulfones in the oxidized samples of **P1** and **P2** were evaluated with infrared spectroscopy and compared to similar spectra for the model compounds (see Figures S3 and S4 in the Supporting

Information). Oxidation causes significant changes in the spectra of both polymers between 1600 and 850 cm⁻¹ (Figure 3). Initially, **P1** has a relatively featureless spectrum. Oxidation with 2.1 equiv of *m*-CPBA causes a strong absorption band at 1077 cm⁻¹ to appear, indicating sulfoxide formation. This band continues to grow and broaden with further oxidation. Beginning with **P1C** and continuing in **P1D**, two peaks at 1335 and 1160 cm⁻¹ belonging to sulfones appear. The FT-IR spectrum of **P2** is more challenging to interpret, because signals between 1150 and 1000 cm⁻¹ from the aryl ether groups interfere with the observation of the sulfoxide band in the oxidized polymers. **P2A**

(25) Stille, J. K.; Whitehurst, D. D. *J. Am. Chem. Soc.* **1964**, *86*, 4871–4876.

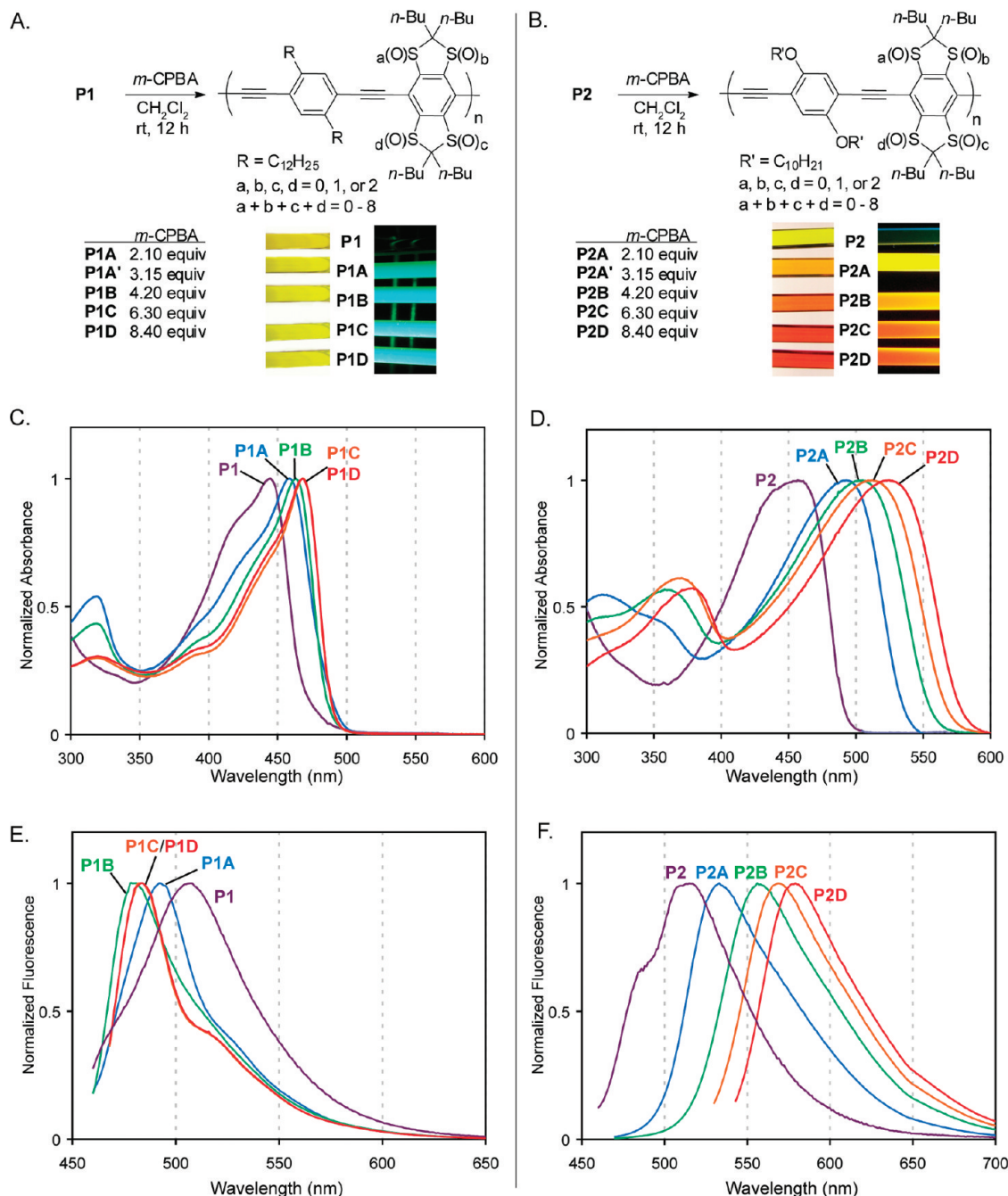


Figure 2. Polymer oxidation. (a and b) The oxidation of **P1** and **P2** with increasing amounts of oxidant is shown. Photographs show solutions of the polymers in CDCl_3 (5 mg/mL) under ambient light (left) and irradiated at 365 nm with a hand-held lamp (right). (c and d) The absorbance spectra of dilute solutions of **P1**, **P1A-D**, **P2**, and **P2A-D** in CH_2Cl_2 are shown. (e and f) The fluorescence spectra of dilute solutions of **P1**, **P1A-D**, **P2**, and **P2A-D** in CH_2Cl_2 are shown and are corrected for PMT response. λ_{ex} : 440–450 nm (**P1**, **P1A-D**), λ_{max} minus 10 nm (**P2**, **P2A-D**).

shows a strong sulfoxide band at 1081 cm^{-1} but does not show sulfone bands. Sulfone bands appear in **P2B** and are accompanied by a decrease in the initial signal belonging to sulfoxides, which suggests that some of the sulfoxides have been oxidized to sulfones. Beginning with **P2C** and continuing in **P2D**, the sulfone peaks at 1335 and 1161 cm^{-1} continue to grow as the sulfoxide signal weakens.

In summary, FT-IR shows that both **P1** and **P2** are first oxidized to sulfoxides and then oxidized to sulfones. **P2** appears to be more easily oxidized to sulfones relative to **P1**, because of its more electron-rich comonomer. It is difficult to comment quantitatively on the level of oxidation using FT-IR; however the spectra support some important qualitative observations. The

P1A and **P2A** spectra suggest that most of the thioether-containing aromatic rings have been oxidized to the disulfoxide, which is in accord with the reactivity seen in the model compounds. The weak sulfone bands seen in **P1D** indicate minimal sulfone formation with 8.40 equiv of oxidant, which suggests that most of the thioether repeating units have four or less oxygen atoms. This is in contrast with the strong sulfone bands observed in **P2D**, which suggest that each thioether repeating unit contains at least four oxygen atoms. In both **P1** and **P2**, the oxidized polymers have complex structures. Although this extra dimension of polydispersity makes characterization challenging, it likely aids in solubility and reduces crystallinity.

Table 2. Polymer Photophysics

polymer	λ_{max} (nm)/ ϵ ($\text{M}^{-1} \cdot \text{cm}^{-1}$) ^a		λ_{em} (nm)		Φ_{F}		τ_{F} ^d (ns)	k_{F} ^e (ns^{-1})	M_{n}^f (kDa)	M_{w}^f (kDa)	PDI ^g
	CH_2Cl_2	film	CH_2Cl_2	film	CH_2Cl_2 ^b	film ^c	CH_2Cl_2	CH_2Cl_2			
P1	444 (44 000)	457	512	517	0.0096	<0.01	0.13	0.074	236 ^h	1990	8.40
P1A	459 (38 000)	464	492	500	0.35	<i>n.d.</i>	0.67	0.52	265	2710	10.2
P1A'	463 (50 000)	<i>n.d.</i>	480	<i>n.d.</i>	0.61	<i>n.d.</i>	0.68	0.90	<i>n.d.</i>	<i>n.d.</i>	<i>n.d.</i>
P1B	463 (54 000)	467	479	498	0.53	0.57	0.73	0.72	215	2010	9.35
P1C	468 (69 000)	469	483	495	0.59	0.70	0.71	0.83	112	587	5.24
P1D	468 (48 000)	468	483	495	0.48	<i>n.d.</i>	0.80	0.60	102	384	3.76
P2	457 (43 000)	489	526	503	0.0085	<0.01	0.17	0.050	18.9 ^h	31.1	1.65
P2A	494 (29 000)	500	532	551	0.49	0.56	1.35	0.36	18.8	32.3	1.72
P2A'	497 (30 000)	<i>n.d.</i>	540	<i>n.d.</i>	0.42	<i>n.d.</i>	1.34	0.31	<i>n.d.</i>	<i>n.d.</i>	<i>n.d.</i>
P2B	503 (25 000)	503	556	580	0.28	<0.10	1.51	0.19	15.9	23.6	1.48
P2C	513 (29 000)	512	568	594	0.25	<0.10	1.66	0.15	13.0	20.3	1.56
P2D	524 (23 000)	520	579	599	0.19	<0.10	1.72	0.11	14.3	22.4	1.57

^a Molar absorptivity based on molecular weight of repeat unit. ^b Absolute quantum yields were determined for **P1**, **P1A–D**, **P2**, and **P2A–B** by comparison with coumarin-6 in ethanol ($\Phi_{\text{F}} = 0.76$). **P2C** and **P2D** were compared to rhodamine B in ethanol ($\Phi_{\text{F}} = 0.49$). ^c Thin-film quantum yields of **P1B**, **P1C**, and **P2A** were determined using an integrating sphere and monochromatic light of several wavelengths near the λ_{max} . Thin-film quantum yields of **P1**, **P2**, **P2B**, **P2C**, **P2D** were determined by comparison with thin films of perylene in PMMA ($\Phi_{\text{F}} = 0.78$). ^d Fluorescence lifetimes were measured using a pulsed-femtosecond laser (350 nm, **P1**, **P2**) or pulsed-picosecond (415 nm, **P1A–D**, **P2A–D**) laser and were fit to monoexponential decays with $R^2 > 0.99$. ^e $\Phi_{\text{F}}/\tau_{\text{F}}$. ^f Determined with GPC(THF) against polystyrene standards. ^g $M_{\text{w}}/M_{\text{n}}$. ^h Degree of polymerization (DP) based on polymer repeat unit is 260 for **P1** and 21 for **P2**.

Optical and Photophysical Properties of the Polymers in Solution. Our primary method of evaluating the effect of oxidation on the polymers is UV–vis and fluorescence spectroscopy (Figure 2, Table 2). **P1** is relatively nonemissive, with a quantum yield less than 0.01. **P1A**'s absorbance ($\lambda_{\text{max}} = 459$ nm) is red-shifted compared to that of **P1** ($\lambda_{\text{max}} = 444$ nm). **P1A**'s emission maximum is blue-shifted from 512 to 492 nm relative to the parent polymer, and its quantum yield increases dramatically (35-fold). When **P1** is treated with 4.2 equiv of oxidant (**P1B**), the absorbance red-shifts and the emission blue-shifts. The spectral changes for **P1B** are accompanied by an increase in quantum yield to 0.53, but the effect of further oxidation is minor.

Similar to **P1**, **P2** is relatively nonemissive in solution, with a quantum yield Φ_{F} of less than 0.01. The quantum yield of **P2A** is 0.49, which represents a more than 49-fold increase in emission when the polymer is treated with 2.1 equiv of oxidant. Additional oxidation causes continued red-shifting in absorbance and emission, as can be seen in **P2B**, **P2C**, and **P2D**. However, greater oxidation is accompanied by a decrease in quantum yield, which appears to be at least partially a result of a decrease in the rate of fluorescence (k_{F}).

Response to Hydrogen Peroxide in Solution. The model compounds and polymers did not react with hydrogen peroxide in solution at room temperature. To facilitate a reaction, the oxidation catalyst methylrhodiumtrioxide (MTO)²⁶ was added as described by Malashikhin and Finney.^{4a} The absorbance and emission of dilute solutions of **MC2** and **P2** in quartz cuvettes were recorded after the addition of catalyst ([MTO] = 0.5 mM) but before the addition of oxidant.²⁷ Following the addition of hydrogen peroxide, the stirred solutions were monitored at 15 min, 3 h, and 20 h. Initially, three solvents were screened (THF, EtOH, DCM), and the extent of reaction was greatest in DCM.

Ethanol showed the same response at a slower rate, but no reaction was observed in THF (unstabilized).

The response at 3 h of a 5.00 μM solution of **P2** to a range of H_2O_2 concentrations is shown in Figure 4. At 3 h, fluorescence increases in the 1.00 mM, 100 μM , 10.0 μM , 1.00 μM , and 100 nM samples but not in the 10.0 nM and 1.0 nM H_2O_2 solutions. The response continues to develop over time, and it can be seen by eye under UV illumination after 20 h (Figure 4, inset picture) for all concentrations of H_2O_2 except 1.00 nM (see Figure S5 in the Supporting Information).

To better understand and characterize the response of **P2** to hydrogen peroxide, a 10.0 μM solution of **MC2** was subjected to similar conditions (see Figure S6 in the Supporting Information). At 15 min, a fluorescence increase is observed in the samples with a H_2O_2 concentration of 1.00 mM, 100 μM , and 10.0 μM . Based on the absorbance spectrum, it appears that after 15 min **MC2** has been transformed to **MC2_2ox** in the 1.00 mM H_2O_2 solution. After 3 h there is no further reaction, indicating that the disulfoxide is a stopping point under these conditions. At 15 min, the 100 μM H_2O_2 solution, which represents 10 equiv of H_2O_2 per molecule of **MC2**, has been oxidized to the monosulfoxide based on the absorbance spectrum. After 3 h, the sample shows further oxidation, though it has not yet reached the same point as the 1.00 mM H_2O_2 solution. The 10.0 μM H_2O_2 solution shows a significant increase in fluorescence at 15 min, but its absorbance spectrum is relatively unchanged. After 3 h, the absorbance spectrum of the 10.0 μM H_2O_2 appears more like that of the monosulfoxide, and the fluorescence has continued to increase. In the 1.00 μM H_2O_2 sample, there is a significant increase in fluorescence, presumably from the formation of some amount of the monosulfoxide, but the absorbance spectrum changes only slightly. The 100 nM H_2O_2 solution shows no response.

Thin-Film Photophysics of Polymers. Thin films of polymers **P1**, **P1A–D**, **P2**, and **P2A–D** were prepared by spin-casting a chloroform solution (1.0 mg/mL) onto silanized glass slides. The films were annealed at 120 $^{\circ}\text{C}$ for 10 min. The films show behavior similar to that of the dilute solutions, with no signs of

(26) (a) Herrmann, W. A.; Kühn, F. E. *Acc. Chem. Res.* **1997**, *30*, 169–180. (b) Vassell, K. A.; Espenson, J. H. *Inorg. Chem.* **1994**, *33*, 5491–5498. (c) Yamazaki, S. *Bull. Chem. Soc. Jpn.* **1996**, *69*, 2955–2959.

(27) **MC1** and **P1** were not investigated because it was anticipated they would respond more slowly to hydrogen peroxide than the more electron-rich **MC2** and **P2**.

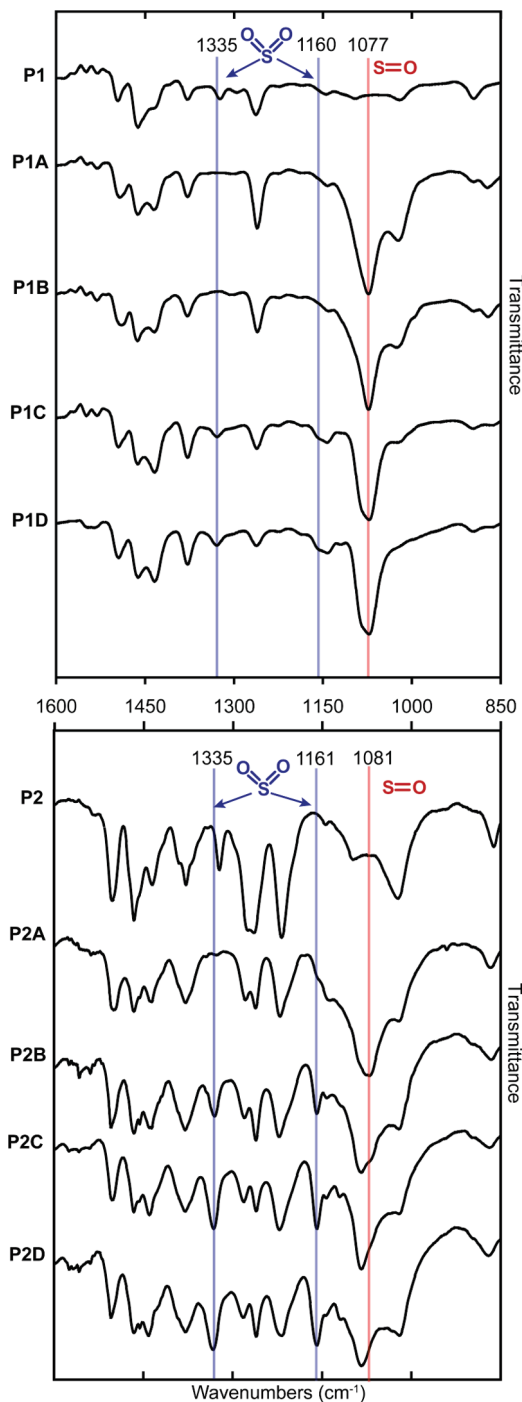


Figure 3. Polymer infrared spectra. A portion of the FT-IR spectra of **P1**, **P1A–D**, **P2**, and **P2A–D** is shown with blue lines indicating sulfone bands and red lines indicating sulfoxide bands. Samples were drop-cast on KBr plates from concentrated CH_2Cl_2 solutions.

aggregation (Table 2, Figure S7 in the Supporting Information). For **P1**, **P1A**, and **P1B**, the thin-film absorption and emission maxima are red-shifted compared to the solution values. For **P1C** and **P1D**, the absorption maxima are relatively unchanged going from solution to thin film; however the emission maxima are red-shifted in the solid state. For **P2** and **P2A**, the thin-film absorption and emission maxima are red-shifted compared to the solution values. **P2B** displays no change in absorption maximum in moving from solution to the solid state; however its emission does red-shift. **P2C** and **P2D** show a slight blue

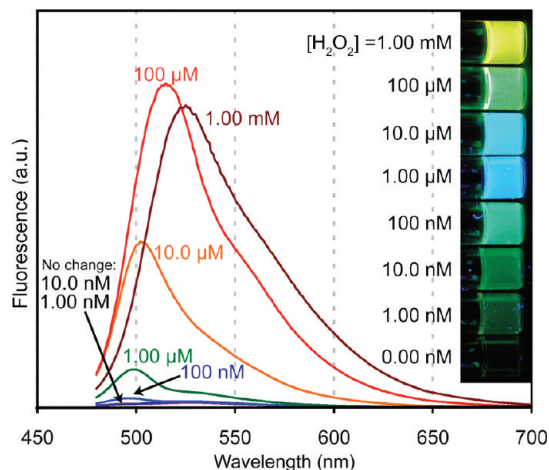


Figure 4. Fluorescence response of **P2** to hydrogen peroxide. The response of **P2** to H_2O_2 after 3 h at room temperature is plotted for a series of hydrogen peroxide concentrations. The inset shows the same solutions under UV irradiation (365 nm) at 20 h. For all solutions: $\lambda_{\text{ex}} = 460$ nm, $[\text{P2}] = 5.00 \mu\text{M}$, $[\text{MTO}] = 0.5$ mM, $[\text{urea}] = [\text{H}_2\text{O}_2]$ in CH_2Cl_2 with $<5\%$ ethanol.

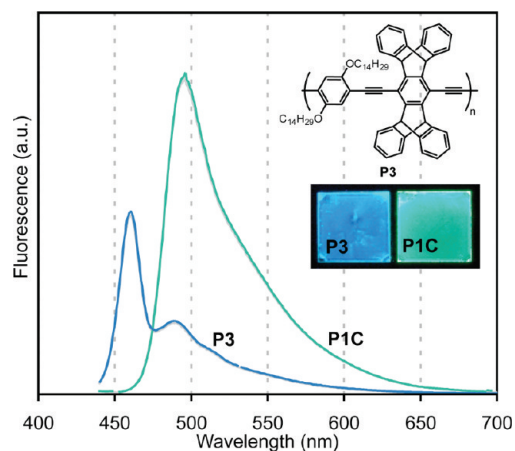


Figure 5. Solid-state emission of **P1C** versus **P3**. The fluorescence emission at an angle of 22.5° to the face of the film is shown for **P3** and **P1C**. The two samples had nearly identical optical densities at the excitation wavelength (420 nm). Representative samples of **P3** and **P1C** under UV irradiation (365 nm) are shown in the inset.

shift in absorption when moving from solution to the solid state; however in both cases the emission is red-shifted.

The films made from the oxidized forms of **P1**, specifically **P1B** and **P1C**, were highly emissive, with quantum yields above 0.50. We compared films of **P1C** to films of a previously reported nonaggregating PPE (**P3**) with a fluorescent quantum yield of 0.33 in the solid state.^{2a} In Figure 5, the emission of **P1C** is significantly greater than that of a film of **P3** when both are excited with a monochromatic light of 420 nm, a wavelength at which the two films have nearly identical optical densities. Films of **P2A** are also highly fluorescent with a quantum yield of 0.56. Comparatively, films of the more highly oxidized polymers (**P2B–D**) are less emissive; however the fluorescence can be clearly seen by eye under UV irradiation as shown in Figure 6.

Thin-Film Photobleaching Studies. Films of **P1**, **P1A–D**, **P2**, and **P2A–D** were tested for photostability by comparing the emissions before and after the films were irradiated at their absorbance maxima for 30 min, using monochromatic light generated from a 450 W steady-state Xe lamp as the irradiation

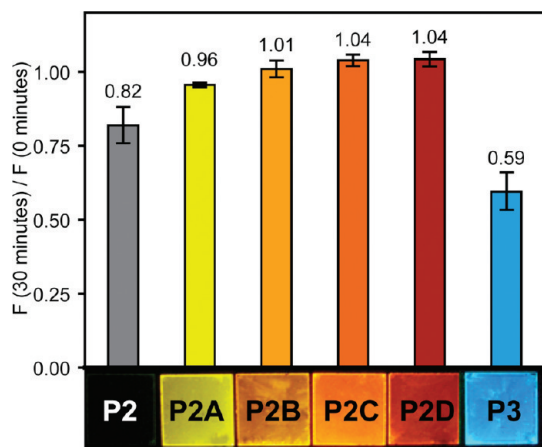


Figure 6. Photostability of **P2** thin films. Thin films of **P2**, **P2A–D**, and **P3** of the same optical density ($OD = 0.05 \pm 0.01$) were irradiated for 30 min at their absorbance maxima with monochromatic light, and the ratio of fluorescence at 30 min to the initial fluorescence was measured. Representative samples under UV irradiation (365 nm) are shown at the bottom of the plot.

source under aerobic conditions.¹¹ The approximate area of irradiation was 0.25 cm^2 and the average power density of irradiation was estimated to be 6 mW/cm^2 . Films of **P1** and **P1A–D** had an optical density (OD) of 0.10 ± 0.01 . Films of **P2**, **P2A–D**, and **P3** had an OD of 0.05 ± 0.01 . The films were not moved during the process to ensure that the measurements reflect the effect of irradiation on one area of the film. All measurements were done in triplicate, and the error is reported as the standard deviation. Films of **P1** and **P1A–D** did not show improved photostability as compared to **P3** under identical conditions¹¹ (see Figure S8 in the Supporting Information). However, films of **P2A–D** proved resistant to photobleaching (Figure 6). **P2A–D** retained more than 95% of their original fluorescence after 30 min of irradiation, with **P2B–P2D** even showing a slight increase in emission. They are more photostable than **P3**, which retains only 60% of its initial emission when irradiated at its absorbance maximum (440 nm) at the same OD , in accordance with previously reported results.¹¹

Discussion

Understanding the Photophysical Behavior of the Model Compounds. Because of its relatively weak intensity, the absorbance band of **MC1** and **MC2** centered at approximately 435 nm (Figure 1) suggests that the thioethers on the center ring impart intramolecular charge transfer (ICT) character to the HOMO–LUMO optical transition. The ICT character of the transition results from poor spatial overlap of the frontier molecular orbitals (FMOs), which we examined with quantum mechanical calculations (Figure 7a, Supporting Information Figure S9).¹⁹ Qualitatively, for **S1** (a simplified version of **MC1** for ease of computation) the HOMO is primarily located on the center ring with most of the orbital density on the sulfur atoms, while the LUMO is delocalized throughout the molecule's π -system with minimal density on the sulfur atoms. The presence of ICT character has been observed in simple thioether containing aromatic compounds, such as phenyl-*n*-propyl sulfide.²⁸ Additionally, ICT character is observed in compound **7**¹⁹ (Chart 1), which is an oxygen analogue of the thioethers studied here.

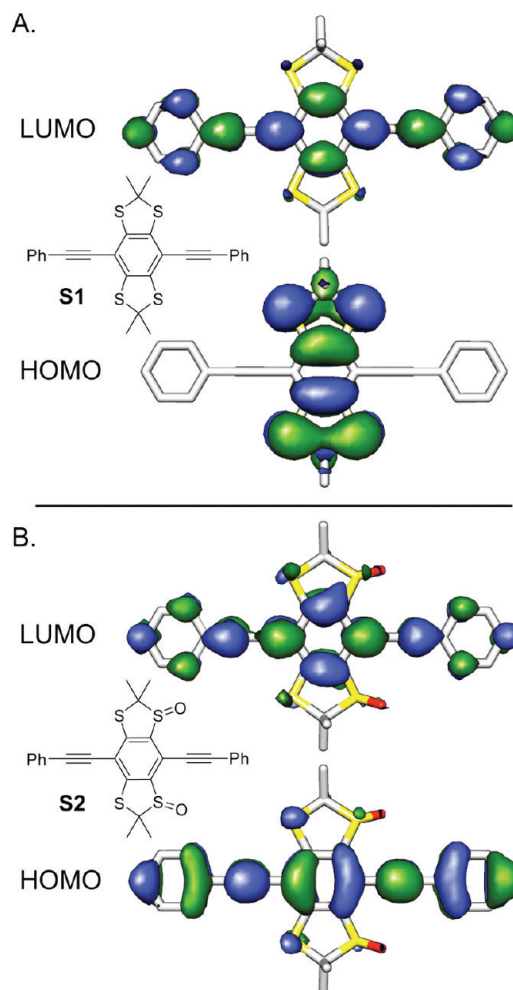


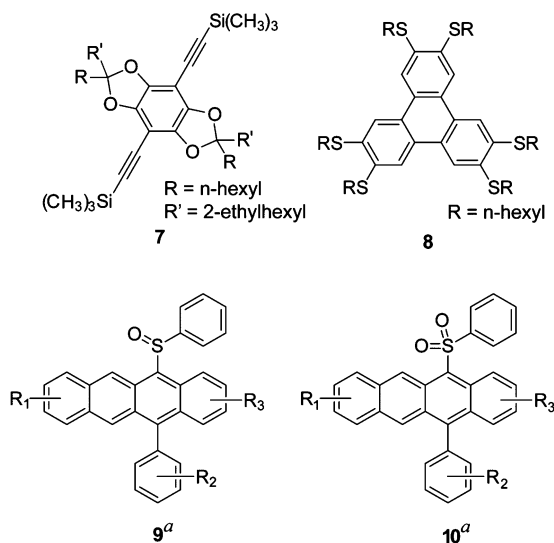
Figure 7. HOMO–LUMO Computations. (a and b) Frontier orbital topologies (B3LYP6-311+G*, Gaussian03) for structures **S1** and **S2**. Structures **S1** and **S2** represent **MC1** and **MC1_2ox_trans**, respectively, with the butyl groups being replaced with methyl groups for ease of computation.

Upon oxidation of **MC1** to **MC1_1ox**, the ICT band blue shifts, and with oxidation to the disulfide, the ICT band disappears. The computed HOMO and LUMO for **S2** are in agreement with this observation, as it appears that the spatial overlap of the HOMO and LUMO is significantly greater for **S2** as compared to **S1** (Figure 7). The situation is more complex in the case of **MC2** and its mono- and disulfides because the oxidation of the thioethers introduces a donor–acceptor interaction between the electron-rich outer rings and the electron-poor middle ring. However, comparing the absorption spectrum of **MC2** to that of **MC2_1ox** reveals that oxidation to the monosulfide causes a blue shift similar to that seen in **MC1_1ox**. The origin of the weak red-shifted absorbance present in both isomers of **MC2_2ox** may be elucidated by future computational studies.

For **MC1** and **MC2**, the fluorescence quantum yield is low in solution ($\Phi_F = 0.003$, Table 1), for two reasons. First, **MC1** and **MC2** have short fluorescence lifetimes of approximately 100 ps, which indicates that another relaxation process is competing with fluorescence. Based on previous studies of thioethers we suggest that intersystem crossing (ISC) from the

(28) Becker, R. S.; Jordan, A. D.; Kolc, J. *J. Chem. Phys.* **1973**, *59*, 4024–4028.

Chart 1. Literature Compounds



^a $R_1, R_2, R_3 = H, \text{OMe}, t\text{-Bu}, \text{Cl}, \text{Br}$.

singlet excited state to the triplet excited state accounts for the shortened lifetime. In compounds as simple as phenyl-*n*-propyl sulfide, ISC is believed to be the predominant deactivation pathway of the excited state.²⁸ An example of an aromatic chromophore containing more than one thioether is 2,3,6,7,10,11-hexakis(*n*-hexylsulfanyl)triphenylene (Chart 1, Compound 8), which has a reduced fluorescence quantum yield compared to the parent triphenylene (0.015 vs 0.066) but displays significant phosphorescence at 77 K.²⁹ Compound 8 has a significantly shortened lifetime (0.7 ns) as compared to the parent triphenylene (36.6 ns) or the same compound with the sulfur atoms replaced by oxygen atoms (8.0 ns). For **MC1** and **MC2**, the observation of room temperature phosphorescence (Figure S1, Supporting Information) in degassed samples further supports the argument that ISC is a main deactivation pathway for the singlet excited state.

The second reason that the unoxidized model compounds have low emission is that they have lower rates of fluorescence (k_F) as compared to the oxidized versions. Oxidation of **MC1** to **MC1_1ox** and both isomers of **MC1_2ox** is accompanied by an increase in k_F . The increase in k_F in the disulfide as compared to the unoxidized compound appears to be a consequence of better spatial overlap between the HOMO and LUMO (see Figure 7).^{23,30} The oxidation of **MC2** to **MC2_1ox** causes the fluorescence lifetime to increase substantially from 0.099 to 2.7 ns but does not increase k_F . Further oxidation to **MC2_2ox** causes an order of magnitude increase in k_F from 0.020 ns⁻¹ to ~0.20 ns⁻¹ and a minor increase in the lifetime.

MC2 shows a more than 150-fold increase in Φ_F when oxidized to the disulfide, but the increase is more modest (7- to 13-fold based on the isomer) when **MC1** is oxidized to the disulfide. We contend that the sulfoxides in **MC1_2ox** are behaving differently than the sulfoxides in **MC2_2ox**. It has been reported that the fluorescence of aromatic sulfoxides is low

because of nonradiative decay pathways involving the sulfoxide. For example, pyrene has a quantum yield of 0.32 in CH₂Cl₂,³¹ and phenyl 1-pyrenyl sulfide has a quantum yield of 0.34 in CH₂Cl₂.^{4a} Oxidation of the sulfur in phenyl 1-pyrenyl sulfide to a sulfoxide causes the quantum yield to decrease to 0.02, whereas further oxidation causes the quantum yield to increase to 0.76.^{4a} A similar trend, in which the presence of a sulfoxide attached directly to an aromatic core quenches a fluorophore that is relatively unaffected by the presence of a thioether or a sulfone in the same position, is observed for naphthalene, biphenyl, and anthracene sulfides.³² However, in the compounds we have examined sulfoxides do not appear to act as fluorescence quenchers except in **MC1_2ox** (and perhaps in **MC1_1ox**), in which case the emission is blue-shifted toward the near-UV. This suggests that when irradiated at higher energies (shorter wavelengths) sulfoxides may quench fluorescence via a mechanism that is not operative at lower energies (longer wavelengths). The behavior of our model compounds and polymers is not unprecedented. Within a previously reported series of 21 tetracene derivatives (Chart 1), 15 of which are sulfoxides (**9**) and 6 of which are sulfones (**10**), the tetracene derivatives with sulfoxides are more emissive than the tetracene sulfones in nearly every case.³³

Understanding the Photophysical Behavior of the Polymers.

In contrast to the model compounds, the HOMO–LUMO optical transitions of **P1** and **P2** appear to be allowed, thus suggesting that the HOMO is partially delocalized along the polymer's π -backbone and has better spatial overlap with the LUMO. In contrast, when the oxygen-containing monomer **7** is incorporated into PPEs the HOMO remains localized.¹⁹ **P1** and **P2**, which like **MC1** and **MC2** are not very emissive, show large increases in Φ_F when oxidized due to an increase in both k_F and τ_F (Table 2). For example, when **P1** is oxidized to **P1A** with 2.1 equiv of oxidant, k_F increases from 0.074 ns⁻¹ to 0.52 ns⁻¹ and τ_F increases from 0.13 to 0.67 ns. When **P2** is oxidized to **P2A**, k_F increases from 0.050 ns⁻¹ to 0.36 ns⁻¹ and the lifetime increases from 0.17 to 1.35 ns. Based on the trends observed for the oxidized model compounds, it appears that the increase in k_F is due to greater spatial overlap of the FMOs due to delocalization of the HOMO along the π -backbone and that the increase in τ_F is due primarily to a decrease in the rate of ISC.

Understanding the Behavior of the Polymers in Thin Films. Because oxidation in solution causes **P1** and **P2** to become emissive, thin films of the thioether-containing polymers were expected to show a fluorescence turn-on response when irradiated in air. However, this phenomenon was not observed. Instead, the already weak emission further decreased with prolonged irradiation (Figure 6, **P2**), even though thioethers are known to react with singlet oxygen.³⁴ There are two possible explanations for this behavior. The first is that the thioethers are not being oxidized to sulfoxides or sulfones under the conditions. The second is that oxidation is so minimal that any oxidized moieties are effectively quenched by the remaining unoxidized segments.

(29) (a) Baunsgaard, D.; Larsen, M.; Harrit, N.; Frederiksen, J.; Wilbrandt, R.; Stapelfeldt, H. *J. Chem. Soc., Faraday Trans.* **1997**, 93, 1893–1901. (b) Marguet, S.; Markovitsi, D.; Millié, P.; Sigal, H. *J. Phys. Chem. B* **1998**, 102, 4697–4710.

(30) Zuccherro, A. J.; Wilson, J. N.; Bunz, U. H. F. *J. Am. Chem. Soc.* **2006**, 128, 11872–11881.

(31) Berlman, I. B. *Handbook of Fluorescence Spectra*; Academic Press: New York, 1965.

(32) (a) Lee, W.; Jenks, W. *J. Org. Chem.* **2001**, 66, 474–480. (b) Jenks, W. S.; Matsunaga, N.; Gordon, M. *J. Org. Chem.* **1996**, 61, 1275–1283.

(33) Lin, Y.; Lin, C. *Org. Lett.* **2007**, 9, 2075–2078.

Blue-Shifted versus Red-Shifted Fluorescence Turn-on Response to H_2O_2 . As discussed in the Results section, both **MC2** and **P2** show a fluorescence turn-on response to oxidation by hydrogen peroxide in the presence of a catalyst (MTO). However, they differ in that **MC2**'s emission blue-shifts and **P2**'s emission red-shifts under these oxidation conditions. As a conjugated polymer, **P2** offers the opportunity for exciton migration along the polymer backbone to the most highly oxidized, and therefore red-shifted, emissive sites.^{2,35} In contrast, each molecule of **MC2** in dilute solution behaves independently. However, **MC2** offers the opportunity for a dark field fluorescence turn-on response.³⁶ A dark field turn-on is when the emissive species is blue-shifted relative to the initial species and, therefore, avoids overlapping emission from the initial species' vibronic manifold of transitions so that there is no initial background signal to subtract. In this situation, the fluorescence turn-on is limited more by the inherent noise in the detector rather than the emissivity of the fluorophore. For example, our instrumentation shows an average turn-on of 900-fold between 430 and 440 nm for **MC2** in 1.00 mM [H_2O_2] after 15 min (see Supporting Information, Figure S6), even though the emission maximum is above 450 nm. In contrast, when **P2** is oxidized there is still substantial emission from the parent polymer to subtract, even though **P2** does show a slight blue shift in emission upon initial oxidation. Therefore, **MC2** offers an advantage in situations where the increase in fluorescence intensity is most important, and **P2** offers an advantage in situations where a change in emission color is desired.

Conclusions

In summary, we have efficiently synthesized model compounds and polymers containing thioethers that show large

increases in fluorescence quantum yield when oxidized. We demonstrate that oxidation is accompanied by a red shift in emission when the compounds contain electron-rich aromatic rings that act as donor groups. Oxidation with hydrogen peroxide in the presence of an organometallic catalyst points to the potential application of these systems in peroxide sensing. Thin films of the oxidized polymers are shown to be very emissive and, in some cases, to have improved photostability. We conclude that oxidation of the sulfur atoms causes an increase in Φ_F by both increasing the rate of fluorescence (k_F) and decreasing the rate of nonradiative decay, thereby increasing the fluorescence lifetime (τ_F). Based on photophysical studies and computation, we propose that the increase in k_F is caused by greater spatial overlap of the frontier molecular orbitals in the oxidized compounds as compared to the unoxidized compounds.

Acknowledgment. We thank Dr. Peter Müller for collecting and solving X-ray crystal structures, Phil Reusswig for help obtaining solid-state quantum yields, and Dr. Jing Zhao of Prof. Mounji G. Bawendi's research group and Casandra Cox of Prof. Daniel G. Nocera's research group for help obtaining fluorescence lifetimes.

Supporting Information Available: Methods, materials, and experimental details. X-ray crystallographic details of compounds **1**, **MC2_1ox**, and **MC1_2ox_cis**. Additional UV/vis and fluorescence spectra, including results of H_2O_2 oxidation of **MC2** and **P2**, and spectra of polymer thin films. FT-IR spectra for **MC1**, **MC2**, and their oxidation products. **P1** photostability results. ^1H and ^{13}C NMR spectra for all previously unreported compounds and polymers. This material is available free of charge via the Internet at <http://pubs.acs.org>.

JA1019063

(34) Clennan, E. L. *Acc. Chem. Res.* **2001**, *34*, 875–884.

(35) Kim, T.-H.; Swager, T. M. *Angew. Chem., Int. Ed.* **2003**, *42*, 4803–4806.

(36) Thomas, S. W., III; Venkatesan, K.; Müller, P.; Swager, T. M. *J. Am. Chem. Soc.* **2006**, *128*, 16641–16648.